

Adaptive Spatial Decorrelator

Seunghyun Min^O, Kwang Bok Lee* and Yong-Hwan Lee*

Samsung Electronics
seunghyun.min@samsung.com

*School of Electrical Engineering and INMC, Seoul National University
klee@snu.ac.kr, ylee@snu.ac.kr.

Abstract

In this paper, an adaptive spatial decorrelator is proposed in smart antenna systems. A spatial decorrelator was proposed in [11] which is similar to a multiterminal receiver, decorrelator in DS/CDMA systems. However, the spatial decorrelator is sensitive to the DOA estimation error. Thus, an adaptive spatial decorrelator is proposed to compensate the DOA estimation error. It uses the equivariant adaptive separation via independence (EASI) algorithm [14] as an adaptation rule. It provides the robustness to the DOA estimation error. The proposed robust beamforming algorithm outperforms the conventional robust beamforming algorithm, such as, the linearly constrained minimum power (LCMP) with diagonal loading and covariance matrix tapering (CMT). And, it operates well even in the high signal-to-noise (SNR) regions.

1. Introduction

An application of smart antenna systems has been suggested in recent years for mobile communications systems to overcome the problem of limited channel bandwidth, thereby satisfying an ever growing demand for a large number of mobiles on communications channels [1], [2]. It has been shown by many studies that when an antenna array is appropriately used in a mobile communications system, it helps in improving the system performance by increasing channel capacity and spectrum efficiency, extending range coverage, tailoring beam shape, steering multiple beams to track many mobiles, and compensating aperture distortion electronically. It also reduces multipath fading, cochannel interferences, system complexity and cost, bit error rates (BER), and outage probability. It has been argued that adaptive antennas and the algorithms to control them are vital to a high-capacity communications system development [3]. Space division multiple access (SDMA) systems are implemented by using smart antenna systems and spatial filtering interference reduction (SFIR).

The need for robust adaptive array beamforming arises in many practical applications where the assumptions on the nature of the signals and/or interference are, to a greater or lesser extent, violated [4]. This need may arise as a consequence of the finite sample support problem, the inherent nonstationary nature of the underlying processes, uncalibrated array manifold errors, or as a consequence of an attempt to reduce real-time computational requirements (or combinations thereof). The perturbation of many array parameters from their ideal conditions under which the theoretical performance of the system is predicted causes degradation in the system performance by reducing the array gain and altering the beam pattern. Quadratic constraints on the weight vector of an adaptive linearly

constraint minimum power (LCMP) beamformer was proposed to improve the robustness to pointing errors and to random perturbations in antenna parameters [5]. However, it still provides the poor performance when the signal-to-noise ratio (SNR) is equal or larger than the interference-to-noise ratio (INR) and both are large ($\geq 10\text{dB}$) [6].

Mailloux [7] and Zatman [8] have independently developed techniques that impart robustness into adapted patterns by judicious choice of null placement and width which is called the covariance matrix taper (CMT) [9]. This approach is indicated when the potential for mismatch exists between the sample support used for adapting (or training) the beamformer and the data to which the weights are applied. Typical causes for this type of nonstationarity include antenna motion and/or vibration, interferer motion (including internal clutter motion), or relatively slow adapted weight update rates ("stale" weights problem) [7], [8]. A more recent cellular communications application where a similar notch-widening technique was successfully employed can be found in [10].

In this paper, an adaptive spatial decorrelator scheme is proposed for SDMA systems. The concept of spatial decorrelator was proposed in [11] which is similar to the linear multiuser receiver, decorrelator in DS/CDMA systems [12], [13]. In [11], the received signal vector is matched filtered to the composite array response matrix which is generated from the DOA estimates. And then, the inverse of the array correlation matrix is multiplied to extract the signals from the spatial matched filter output vector. However, this scheme is sensitive to the DOA estimation error because the interference signals cannot be nulling. To overcome these problems, the adaptively implemented spatial decorrelator is proposed. The proposed scheme uses the equivariant adaptive separation

via independence (EASI) algorithm [14]. This algorithm is serially updated the weight vectors and uses the relative gradient descent for adaptation rules. The adaptation process is conceptually composed of two steps, whitening process and orthogonal process.

This paper is organized as follows. In section 2, the system models are shown. The spatial decorrelator is explained in section 3, and the proposed adaptive spatial decorrelator is explained in section 4. Numerical results are shown in section 5 and conclusions are drawn in section 6.

2. System model

Consider a uniform linear array with N half-wavelength spaced antenna elements. Thus, the received signal at the n^{th} antenna may be represented as

$$x_n(t) = \sum_{k=1}^K e^{j(n-1)\pi \sin \theta_k(t) + \phi_k} s_k(t) + v_n(t). \quad (1)$$

where K is the number of sources, $\theta_k(t)$ is the DOA of the k^{th} sources, ϕ_k is the carrier phase which is uniformly distributed in $[0, 2\pi]$, $s_k(t) = \sum_{i=-\infty}^{\infty} d_k(i)p(t-iT-\tau_k)$, $d_k(i)$

is the transmitted data, $p(t)$ denotes the pulse shaping waveform, $v_n(t)$ is the additive white Gaussian noise, τ_k and T is the time delay and the symbol interval, respectively. It is assumed that the SDMA systems environments. We may write the received signals in vector form

$$\mathbf{x}(t) = \mathbf{A}(\boldsymbol{\theta}(t))\mathbf{S}(t) + \mathbf{v}(t) \quad (2)$$

- $\mathbf{x}(t) = [x_1(t) \ x_2(t) \ \dots \ x_N(t)]^T$ is an $N \times 1$ vector of received signals at time t where the superscript T denotes the vector transpose;
- $\boldsymbol{\theta}(t) = [\theta_1(t) \ \theta_2(t) \ \dots \ \theta_K(t)]^T$ is the source DOA parameter vector;
- $\mathbf{A}(\boldsymbol{\theta}(t))$ is the composite array response matrix which is determined by the DOA of signals. The k^{th} column of $\mathbf{A}(\boldsymbol{\theta}(t))$ is defined as the array response vector associated with the k^{th} source and is given by $\mathbf{a}(\theta_k(t)) = [e^{j0} \ e^{-j\pi \sin \theta_k(t)} \ \dots \ e^{-j(N-1)\pi \sin \theta_k(t)}]^T$;
- $\mathbf{S}(t) = \text{diag}[s_1(t)e^{j\phi_1} \ s_2(t)e^{j\phi_2} \ \dots \ s_K(t)e^{j\phi_K}]$;
- $\mathbf{v}(t) = [v_1(t) \ v_2(t) \ \dots \ v_N(t)]^T$ is an $N \times 1$ additive noise vector, which is assumed to be spatially and temporally white Gaussian.

3. Spatial decorrelator

Figure 1 shows the block diagram of the spatial decorrelator. The received signal vector is matched filtered to the estimated composite array response matrix which is generated from the DOA estimates. The output of the matched filtered vector, $\mathbf{z}(i)$ may be represented as

$$\mathbf{z}(i) = \mathbf{A}^H(\hat{\boldsymbol{\theta}}(i))\mathbf{x}(i) = \mathbf{A}^H(\hat{\boldsymbol{\theta}}(i))\mathbf{A}(\boldsymbol{\theta}(i))\mathbf{S}(i) + \mathbf{A}^H(\hat{\boldsymbol{\theta}}(i))\mathbf{v}(i) \quad (3)$$

When it is assumed that the DOA estimation for each user is perfect, the transmitted data may extracted from $\mathbf{z}(i)$ by multiplying the inverse of the array correlation matrix \mathbf{R}_{corr}

which is defined as $\mathbf{R}_{\text{corr}} = \mathbf{A}^H(\boldsymbol{\theta}(i))\mathbf{A}(\boldsymbol{\theta}(i))$ as follows

$$\mathbf{y}(i) = \mathbf{R}_{\text{corr}}^{-1} \mathbf{z}(i) = \mathbf{S}(i) + \mathbf{R}_{\text{corr}}^{-1} \mathbf{A}^H(\hat{\boldsymbol{\theta}}(i))\mathbf{v}(i). \quad (4)$$

However, when there is the DOA estimation error, the inverse of the estimated array correlation matrix cannot null the interference signals. Hence, the performance of the spatial decorrelator is degraded.

Figure 2 shows the spatial decorrelator performance as a function of the DOA estimation error when the number of user is 3 and signals are located in $-45^\circ, 0^\circ, 30^\circ$ and the DOA estimation occurs at the signal sources at 0° . As shown in Fig. 2, the signal-to-interference-plus-noise ratio (SINR) decreases as the DOA estimation error increases. When the SNR is low, the effect of the DOA estimation error is small because is noise power is more dominant than the residual interference power. However, when SNR is high, the residual interference signal power is dominant in the SINR performance. Thus, the sensitivity to the DOA estimation error increases as the SNR increases. Thus, the robustness of the beamforming algorithm to the DOA estimation error is required in the high SNR environments.

4. Adaptive spatial decorrelator

In this section, the adaptively implemented spatial decorrelator is proposed. Figure 3 shows the block diagram of the adaptive spatial decorrelator.

From (3), when there is the DOA estimation error, the spatial matched filtered output may be rewritten as

$$\mathbf{z}(i) = \mathbf{A}^H(\hat{\boldsymbol{\theta}}(i))\mathbf{A}(\boldsymbol{\theta}(i))\mathbf{S}(i) + \mathbf{A}^H(\hat{\boldsymbol{\theta}}(i))\mathbf{v}(i).$$

Thus, the purpose of the adaptive spatial decorrelator is adaptively implementing the $(\mathbf{A}^H(\hat{\boldsymbol{\theta}}(i))\mathbf{A}(\boldsymbol{\theta}(i)))^{-1}$.

In this paper, the equivariant adaptive separation via independence (EASI) algorithm is adopted to implement the adaptive spatial decorrelator. This algorithm is serially updated the weight vectors and uses the relative gradient descent for adaptation rules.

The weighting matrix $\mathbf{W}(i)$ is updated according to

$$\mathbf{W}(i+1) = \mathbf{W}(i) - \lambda_i H(\mathbf{y}(i))\mathbf{W}(i) \quad (5)$$

where $\mathbf{y}(i)$ is the output of the $\mathbf{W}(i)$, λ_i is a sequence of positive adaptation steps, and $H(\cdot)$ is K by K matrix used for the updating $\mathbf{W}(i)$.

As mentioned previously, the EASI algorithm composed of the two steps, whitening process and orthogonal process. From the whitening process, the requirement is

$$E[\mathbf{y}\mathbf{y}^H] = \mathbf{I}. \quad (6)$$

(6) means that the output \mathbf{y} is spatially white. This condition ensures second-order independence (i.e. decorrelation) of the separated signal. However, it is not sufficient for determining a weighting matrix since if the output \mathbf{y} is further rotated by some orthogonal matrix, the condition $\mathbf{R}_y = \mathbf{I}$ is preserved, but the signal separation is no longer achieved. Hence, something other than second-order conditions are required; these are provided by the skew-symmetric condition

$$E[\mathbf{g}(\mathbf{y})\mathbf{y}^H - \mathbf{y}^H \mathbf{g}(\mathbf{y})] = \mathbf{0} \quad (7)$$

If the component of \mathbf{y} are mutually independent, the for $i \neq j$, one has $E[y_i g_j(y_j)] = E[y_i]E[g_j(y_j)] = 0$, where the first equality is by the independence assumption and the

second equality by the zero mean assumption. It follows that the off-diagonal entries of matrix $E[\mathbf{y}\mathbf{g}^H(\mathbf{y})]$ are zero, and consequently, (7) is satisfied if $\mathbf{W}(i)$ is a separating weighting matrix. Hence, the separating weight matrix $\mathbf{W}(i)$ may be updated as follows

$$\mathbf{W}(i+1) = \mathbf{W}(i) - \lambda(i)[\mathbf{y}\mathbf{y}^H - \mathbf{I} + \mathbf{g}(\mathbf{y})\mathbf{y}^H - \mathbf{y}^H \mathbf{g}(\mathbf{y})]\mathbf{W}(i) \quad (8)$$

where $\mathbf{g}(\mathbf{y})$ is the component-wise nonlinear function. The nonlinear function g_i are restricted to be phase-preserving, i.e., of the form

$$g_i(y_i) = y_i l_i(|y_i|^2) \quad 1 \leq i \leq K \quad (9)$$

where the l_i 's are real-valued functions. In this dissertation, $g_i(y_i) = y_i |y_i|^2$ is used for the nonlinear function.

5. Numerical results

It is investigated that the performance of the adaptive spatial decorrelator and the LCMP with diagonal loading. It is assumed that the number antenna element, N is 8, the number of signal sources is 3. The signal sources are located in $-45^\circ, 0^\circ, 30^\circ$. In this section, the performance of the robust beamforming algorithm is shown by computer simulations. In the adaptive spatial decorrelator, the step size is set to 0.0001 and the SINR is measured in the steady state interval. The weighting matrix is updated by using (3.30). In the LCMP with diagonal loading, the weight vector is calculated by using in [5], and the covariance matrix is modified by using in [9] for the CMT.

Figure 4 shows the SINR performance of the adaptive spatial decorrelator, LCMP with diagonal loading and for different loading-to-noise ratio (LNR), and CMT with diagonal as a function of DOA estimation error. Fig. 4 (a) shows the SINR performance when SNR=0dB. The proposed adaptive spatial decorrelator shows the robustness according to the DOA estimation error. In the LCMP without diagonal loading, the performance degradation is serious as the DOA estimation error increases because the beamformer cancels the desired user signals due to the DOA estimation error. As the LNR increases the robustness approaches to the adaptive spatial decorrelator. And, the CMT with diagonal with 30dB loading case is similar to the LCMP with 30dB diagonal loading case. Fig. 4 (b) shows the SINR performance when SNR=30dB. The proposed adaptive spatial decorrelator also shows the robustness according to the DOA estimation error. In the LCMP with diagonal loading, as the LNR increases the robustness increases. However, the performance gap between the adaptive spatial decorrelator and the LCMP with diagonal loading is somewhat large in comparison to the SNR=0dB case. As mentioned previously, the worst case for the LCMP with diagonal loading is when the SNR \geq INR and both are large (≥ 10 dB). However, this environment frequently occurs because the high level modulation scheme is adopted in wireless communications which requires the high SNR. Therefore, the robustness of the proposed adaptive spatial decorrelator is important. And, the CMT effect shows when the number of antenna elements becomes large. Thus, in this simulation, the CMT effects is not shown.

6. Conclusions

The adaptive spatial decorrelator is proposed in the paper. The adaptive spatial decorrelator is similar to the multiuser receiver, decorrelator in DS/CDMA systems. The received signal vector is correlated with the estimated array response matrix. The weight matrix is trained to make the output of the adaptive spatial decorrelator independent. It uses the EASI algorithm for adaptation which is based on the serial update and the relative gradient descent. The EASI algorithm is composed of the two steps, whitening process and orthogonal process. The proposed adaptive spatial decorrelator is robust to the DOA estimation error even in the high SNR environments because the SINR loss in comparison with the perfect DOA estimation case is 0.6dB at SNR=30dB for adaptive spatial decorrelator and 24dB for the LCMP with DL and CMT.

References

- [1] L. C. Godara, "Application of Antenna Arrays to Mobile Communications, Part I: Performance Improvement, Feasibility, and System Considerations," *Proc. IEEE*, vol. 85, no. 7, pp. 1031-1060, Jul. 1997.
- [2] L. C. Godara, "Application of Antenna Arrays to Mobile Communications, Part II: Beam-Forming and Direction-of-Arrival Consideration," *Proc. IEEE*, vol. 85, no. 8, pp. 1195-1245, Aug. 1997.
- [3] T. S. Rappaport, "Wireless personal communications: Trends and challenges," *IEEE Antenna Propagat. Mag.*, vol 33, pp. 19-29, Oct. 1991.
- [4] E. J. Kelly, "Adaptive detection in nonstationary interference, Part III," Tech. Rep. 761, Mass. Inst. Technol. Lincoln Lab., Lexington, Aug. 1987.
- [5] Z. Tian, K. L. Bell, and H. L. Van Trees, "A Recursive Least Squares Implementation for LCMP Beamforming Under Quadratic Constraint," *IEEE Trans. Signal Processing*, vol. 49, pp.1138-11145, Jun. 2001.
- [6] H. L. Van Trees, *Optimum Array Processing: Part IV of Detection, Estimation, and Modulation Theory*, John Wiley & Sons, Inc., New York.
- [7] R. J. Mailloux, "Covariance matrix augmentation to produce adaptive array pattern troughs," *Electron. Lett.*, vol. 31, no. 10, pp. 771-772, 1995.
- [8] M. Zatman, "Production of adaptive array troughs by dispersion synthesis," *Electron. Lett.*, vol. 31, no. 25, pp. 2141-2142, 1995.
- [9] J. R. Guerci, "Theory and Application of Covariance Matrix Tapers for Robust Adaptive Beamforming," *IEEE Trans. Signal Processing*, vol. 47, no. 4, pp. 977-985, Apr. 1999.
- [10] J. Riba, J. Goldberg, and G. Vazquez, "Robust beamforming for interference rejection in mobile communications," *IEEE. Trans. Acoust., Speech, Signal Processing*, vol. 45, pp. 271-275, Jan. 1997.
- [11] S. Y. Miller and S. C. Schwartz, "Integrated Spatial-Temporal Detectors for Asynchronous Gaussian Multiple-Access Channels," *IEEE Trans. Commun.*, vol 43, no. 2/3/4, pp. 396-411, Feb./Mar./Apr. 1995.

- [12] R. Lupas and S. Verdú, "Linear multiuser detectors for synchronous code-division multiple-access channels," *IEEE Trans. Inform. Theory*, vol. 35. no. 1, pp.123-136, Jan. 1989.
- [13] R. Lupas and S. Verdú, "Near-far resistance of multiuser detectors in asynchronous channels," *IEEE Trans. Commun.*, vol. 38. no. 4, pp. 496-508, Apr. 1990.
- [14] J.-F. Cardoso and B. H. Laheld, "Equivariant Adaptive Source Separation," *IEEE Trans. Signal Processing*, vol. 44, no. 12, pp. 3017-3030, Dec. 1996.

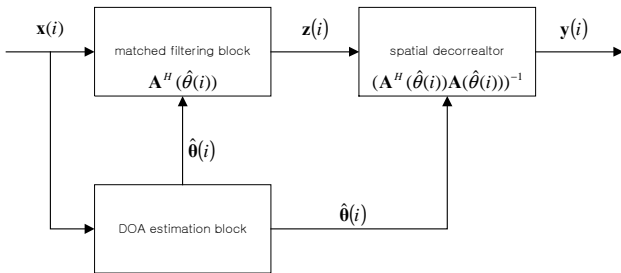


Fig. 1. Block diagram of the spatial decorrelator

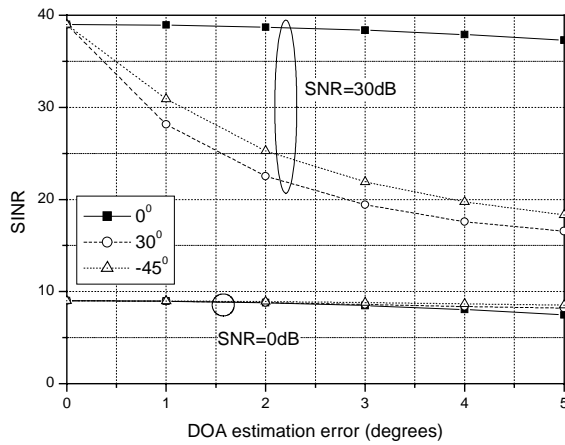


Fig. 2. Performance of the spatial decorrelator

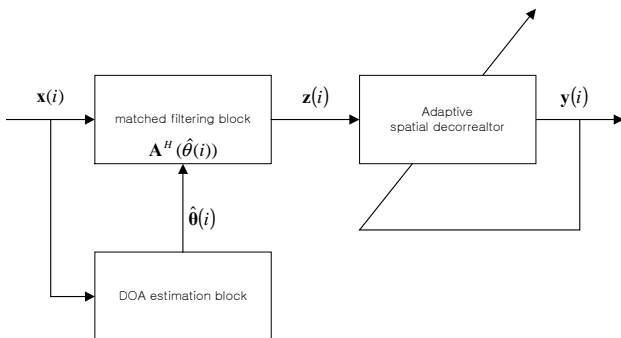
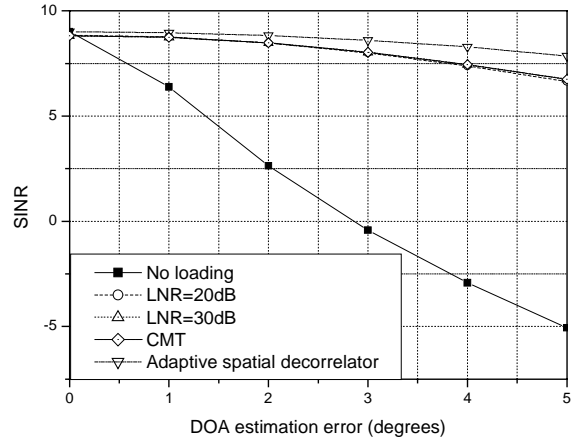
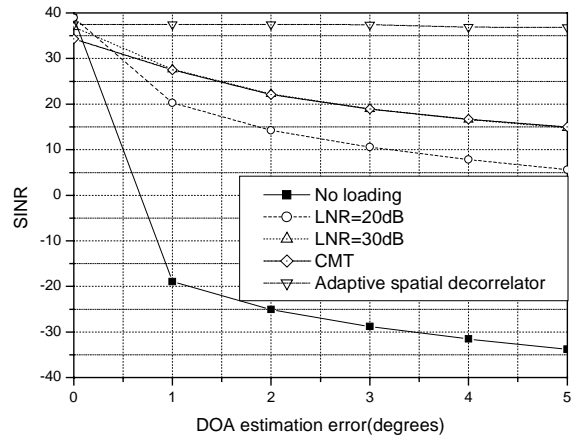


Fig. 3. Block diagram of the adaptive spatial decorrelator



(a) SINR performance (SNR=0dB)



(b) SINR performance (SNR=30dB)

Fig. 4. Performance of the robust beamforming algorithm